



## Effect of Synthesis Approach on Characteristics of CZTS Kesterite Layers for Photovoltaic Applications.



Laila Saad\*, Naglaa Farag, and Doaa Shehata, Mai F. Hamam

Department of Renewable Energy Science and Engineering, Faculty of Postgraduate Studies for Advanced Sciences (PSAS), Beni-Suef University, 62511 Beni-Suef, Egypt.

### Abstract

The final features of the copper zinc tin sulfide (CZTS) kesterite absorber layer is significantly influenced by the preparation method, the resulting layer shape, structure, and electrical characteristics are closely related. The objective of this study is to optimize the operating conditions for the different preparation technique and to study their effects on the final characteristics of kesterite CZTS absorber layers. Three alternative methodological approaches are used and optimized to produce kesterite layers: hot injection, spray pyrolysis, and sol-gel techniques. Snow-crystal shapes, flower-petal shapes, and nanochannel shapes are some of the layer morphologies that have been observed. These morphologies clearly and directly affect other qualities, especially electrical properties. The synthesized CZTS layers exhibit carriers' concentrations values ranging from  $3.2078 \times 10^{14}$  to  $1.7248 \times 10^{22}$  which are relatively higher than the reported values. CZTS layer prepared with spray pyrolysis technique has a higher carrier concentration value than the reported values, the reason for this behavior may be due to the absence of the undesired secondary phases. The preparation technique plays a key role in the final characteristics of the CZTS kesterite layer, with spray pyrolysis and sulfurization resulting in high conductive characteristics and enhanced carriers' concentration and conductivity values.

**Keywords:** CZTS Kesterite; Morphology; synthesis techniques; electric characteristics.

### 1. Introduction

One of the most abundant forms of energy on Earth is solar radiation, but harnessing it has been hampered by the high costs of present solar technologies.<sup>1</sup> These prices are the result of using subpar (silicon), toxic (cadmium), and expensive (indium) components. To further reduce the cost of solar energy, earth-friendly, non-toxic, and economical materials that can compete with fossil fuels are required.<sup>2</sup> Copper zinc tin sulphide is a quaternary semiconducting compound that has gained popularity as absorber layer in thin film solar cells.<sup>3</sup> As well as other I<sup>2</sup>-II-IV-VI<sub>4</sub>-related materials include copper zinc tin selenide and the sulfur-selenium alloy CZTSSe, due to their earth-abundant, economical, non-toxic components and good material qualities, has already been demonstrated to be an excellent choice for use in thin-film solar cells.<sup>4</sup> The second generation solar cells (thin-film technology) was developed in reaction to the excessive material consumption and expenses associated with silicon

sun cells.<sup>5</sup> This entails using materials with high absorption coefficients to decrease the amount of material required.<sup>6, 7</sup> It is also concentrating on employing polycrystalline materials and processes to further reduce prices. However, this cost-cutting has resulted in a reduction in overall efficiency.<sup>5, 7, 8</sup> This technology is now being commercialised with two material systems: cadmium telluride (CdTe) and copper indium gallium selenide (CIGS).<sup>5, 9, 10</sup> While CdTe and CIGS solar cells are the most affordable on the market, both Indium and Gallium, which are used in CIGS, have significant downsides.<sup>10, 11, 12</sup> The goal of this study is to optimize the preparation parameters for the CZTS layer using various solution processing methods to investigate the effect of preparation conditions on the layers structures, morphologies, and electrical properties.

### 2. Methods

#### Materials

Copper Chloride, Zinc Acetate, Tin Chloride, Sulphur, Oleyamine, Copper acetate monohydrate, Zinc acetate dihydrate, sulfur, Ethanol, Tin chloride

\*Corresponding author E-mail: [laila.saad.h@gmail.com](mailto:laila.saad.h@gmail.com); (Laila Saad)

Receive Date: 11 August 2023 Revise Date: 18 September 2023 Accept Date: 23 September

DOI: 10.21608/EJCHEM.2023.228636.8410

©2024 National Information and Documentation Center (NIDOC)

mono hydrate, Thiourea, 2-methoxyehanol, Mono ethanol amine and hydrochloric acid.

### **CZTS Synthesis via Hot Injection Technique**

For the preparation of S precursor, 0.32 g of sulphur was added to 10 ml of oleylamine and sonicated for 30 min at 70 °C. From this freshly prepared sulphur solution. Copper chloride (1.7 mmol of Cu), zinc acetate (1.08 mmol of Zn), tin chloride (0.9 mmol of Sn) were added to 12 ml of oleylamine and mixed in a three-neck flask followed by stirring the solution for 1 hour at 170°C in a nitrogen atmosphere. After stirring, the temperature was increased gradually and the color of the mixture was changed from blue to brown-yellow.<sup>13</sup> A second solution was prepared by adding 0.32 g of sulphur was mixed with 10 ml of oleylamine to yield the S precursor (4.5 mmol of S), which was then sonicated for 30 minutes at 70 °C. At the point when the temperature of the first mixture reached 230 °C, the second solution was injected and the CZTS ink was formed. For precipitating the CZTS ink particles, toluene was rapidly added to the mixture. For washing and purifying the product, ethanol was added to the product and it was sonicated for 30 minutes to ensure the complete dispersion. The solution was then centrifuged at 4000 rpm for 30 minutes. The previous process was repeated three times for removing the unreacted solvents and any other by-products. The final CZTS product was obtained in the form of a stable ink solution. CZTS films were prepared by drop-casting on glass substrates followed by annealing at 250 °C.

### **CZTS Synthesis via Spray pyrolysis technique**

Copper chloride dihydrate (0.1 M), zinc acetate (0.1 M), tin chloride (0.1 M), and thiourea (0.8 M), were added into a solvent mixture of acetic acid (20 ml), distilled water (30 ml), and ethanol (50 ml) by the ratio (2:3:5).<sup>14</sup> The solution was stirred for an hour to prevent any deposits.<sup>15</sup> After completing this process, a yellow solution is formed. The glass substrates were washed with 5% HNO<sub>3</sub> and then rinsed with distilled water and ethanol. The substrates were heated up at a temperature of 300 °C and the CZTS solution was then sprayed on the heated glass substrates via a spray gun using an air compressor. The distance between the nozzle and the substrate is kept to 20cm. The prepared films had surfaced with a bad homogeneity because of the discontinuous spraying patches and the large size of the gun droplets. So, the sprayer was replaced by a nebulizer under the same conditions. The prepared films were uniform and homogenous this may be due to the nebulizer spraying the solution as well as distributed fog. The prepared thin films were annealed at 320° for 12 hours.

### **CZTS Synthesis via Sol-gel Technique**

In this method, copper acetate monohydrate (0.46 mol/L), zinc acetate dihydrate (0.27 mol/L), tin chloride monohydrate (0.27 mol/L) and thiourea (2 mol/L) were dissolved in 2-methoxyehanol and mono ethanol amine as a stabilizer.<sup>16</sup> Few drops of diluted HCl were added to the solution to control the pH of the solution.<sup>13</sup> The mixture was stirred on a hot plate magnetic stirrer at 50 °C for 8 hours. The procedures were performed at two different pH values: 8 and 10 in order to study the effect of the pH on the structural, physical and electrical properties of the prepared CZTS layers. The prepared CZTS solution was deposited on cleaned substrates by a dip coater device with a speed of 150 mm/ minute, then the wet films were dried on a hot plate at 200 °C for 5 minutes. The deposited films were exposed to sulfurization process at a tubular quartz furnace at 560 °C for 3 min in a sulfur atmosphere.

## **3. Results**

### **Structural Characteristics of the CZTS**

The structures of the CZTS films were investigated using X-ray diffraction patterns (XRD). XRD analysis of the CZTS thin film samples which prepared using hot injection method, spray pyrolysis and sol-gel techniques are shown as stack in Figure 1, respectively. For all the investigated samples, the four main peaks of CZTS and/or ZnS phase are observed near 28°, 33°, 47° and 56° according to the decreasing intensity order, which matches the standard JCPDS cards no. 01-071-5976 and no.00-26-0575 for ZnS and CZTS respectively.<sup>17</sup> for spray pyrolysis sample, copper sulfide (Cu<sub>2</sub>S) peaks are observed also and matches the JCPDS card no. 00-053-0522 for cubic copper sulfide (Cu<sub>2</sub>S), which observed at 46.3, 32.4, and 54.3°.<sup>18</sup> The appearance of those peaks suggested the presence of an undesired secondary phases of ZnS and/or Cu<sub>2</sub>S.<sup>18</sup> The crystallite sizes (D) of CZTS particles were calculated using Scherrer's formula. Crystallite size of all samples was calculated corresponding to most intense peak (112). Crystallite size of CZTS prepared via hot injection, spray pyrolysis and sol-gel techniques were 5, 30 and 20 nm, respectively.

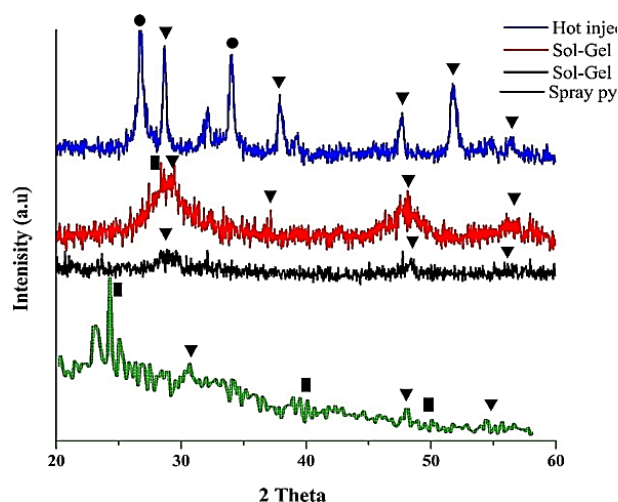


Figure (1): XRD patterns of CZTS film synthesized by hot injection, Sol-gel (PH 8 and PH 10), and spray pyrolysis techniques, where  $\nabla$  = CZTS,  $\blacksquare$  = Secondary phase, and  $\bullet$  = FTO substrate.

### Morphologies Studies of the CZTS layers

The observed morphologies of the different CZTS layers via scanning electron microscope (SEM) shows that the CZTS layer which was synthesized via hot injection method exhibits a randomly grown "flower petal"-like morphology with no appearance of the undesired cubic secondary phases as represented in Figure 2(a). However, for the CZTS layer prepared by spray pyrolysis technique, shows a micro-channel consisting of accumulated nanoparticles where the sizes of the particles are ranged from 20 to 30 nm, Figures 2(b).

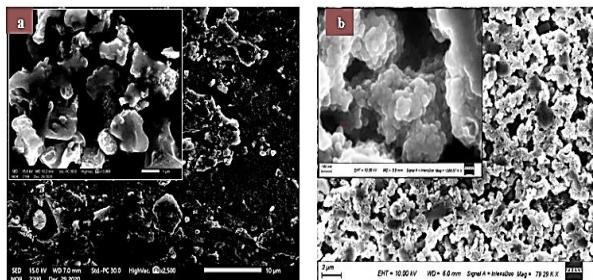


Figure (2) Surface morphologies of CZTS film synthesized by: a) hot injection, and b) spray pyrolysis techniques.

### Electrical characteristics of the CZTS layers

The carrier mobility, conductivity, and carrier concentrations of CZTS thin films were measured by Hall effect and are summarized in Table I. The CZTS layers are functioning as p-type thin films resulting from the positive sign of the Hall coefficient. The typical carrier concentration of CZTS is in the range of ( $\sim 10^{16}$ – $10^{17}$  cm<sup>-3</sup>). Herein, the synthesized CZTS layers exhibit carriers' concentrations values ranging from  $3.2078 \times 10^{14}$  to  $1.7248 \times 10^{22}$  which are relatively higher than the reported values.<sup>19, 20</sup>

CZTS layer prepared with spray pyrolysis technique has a higher carrier concentration value than the reported values, the reason for this behavior may be due to the absence of the undesired secondary phases which result from using a nebulizer in the spraying process. For the CZTS samples prepared via the sol-gel technique, the sulfurization process of the CZTS enhanced the carriers' concentration by several orders of magnitude as well as the conductivity values. This behavior may be due to the sulphur that passivate the CZTS surface and decrease both the surface trap and the carriers' recombination. However, the carrier mobility was enhanced for the sample prepared at PH8 and deteriorated for the sample prepared at pH 10.

Table I: The electrical parameters of the prepared CZTS layers

Sample CZTS (Preparation Technique)		Carriers density [cm <sup>-3</sup> ]	Conductivity [ $\Omega^{-1}$ cm <sup>-1</sup> ]	Carrier mobility [cm <sup>2</sup> /Vs]	
Spray Pyrolysis		$2.6 \times 10^{20}$	$7.6037 \times 10^4$	$1.826 \times 10^3$	
Hot injection		$3.1 \times 10^{18}$	$2.3944 \times 10^2$	$4.7974 \times 10^2$	
Sol-gel	pH 8	before sulphurization	$3.2 \times 10^{14}$	$3.3347 \times 10^{-4}$	6.4874
		after sulphurization	$3.6 \times 10^{19}$	$1.7517 \times 10^2$	30.645
	pH 10	before sulphurization	$2.6 \times 10^{15}$	$7.6473 \times 10^2$	$1.8762 \times 10^2$
		after sulphurization	$1.7 \times 10^{22}$	$3.4145 \times 10^4$	12.357

### Discussion

#### Effect of Sulfurization (annealing process)

Only metal binaries, such as Cu<sub>5</sub>Zn<sub>8</sub>, Cu<sub>6</sub>Sn<sub>5</sub>, CuZn, and Cu<sub>3</sub>Sn may be produced at ambient temperature.<sup>21</sup> Metal chalcogenide binaries such as CuX, Cu<sub>2</sub>X, and SnX are generated between 200 and 450 degrees Celsius, while CuX binaries react with Sn to form Cu<sub>x</sub>SnS between 450 and 500 degrees Celsius.<sup>1</sup> ZnX interacts with Cu<sub>2</sub>SnX<sub>3</sub> to create Cu<sub>2</sub>ZnSnX<sub>4</sub> at higher temperatures between 550 and 580 °C, and for an annealing duration of 8 h or one-step deposition at 500 °C, according to the equation:  $\text{Cu}_2\text{SnX}_3 + \text{ZnX} \rightarrow \text{Cu}_2\text{ZnSnX}_4$ . Eq. (1)<sup>1</sup>

The temperature is crucial during the film deposition process. To regulate which reaction occurs during the annealing/sulfurization process, the temperature of the layers must be constantly monitored. Fast annealing (a few minutes) is adequate for two-step procedures utilising elemental sulphur. Herein the sulfurization process of the deposited films achieved at a tubular quartz furnace at 560 °C for 3 min in a sulfur atmosphere.<sup>1</sup> A significant effect of the sulfurization process on the morphology of CZTS which is synthesized by the sol-gel technique was

noticed using SEM. Before the sulfurization process, the surface morphology of the CZTS displayed “snow crystals”-shaped, Figure (3 A-D). When of one of the snow crystal-shaped arms was etched by the electron beam (12 KV), a fine connected network appeared from underneath the crust of the large crystals, Figure (3 E and F). After undergoing the sulfurization process the snow crystals shaped were totally ruptured Figure (5)E and (F) and the connected network can be clearly observed as shown in Figure(4). This revealed connected network is expected to work as a channel to facilitate the charge transfer and therefore increase the carrier’s mobility. The investigated morphological transformation manifests the importance of the sulfurization process after sol-gel synthesis of CZTS. On the other hand, Figure (5) displays the appearance of a few secondary phases which are undesired and can be attributed to the temperature change during the preparation process.<sup>21</sup>

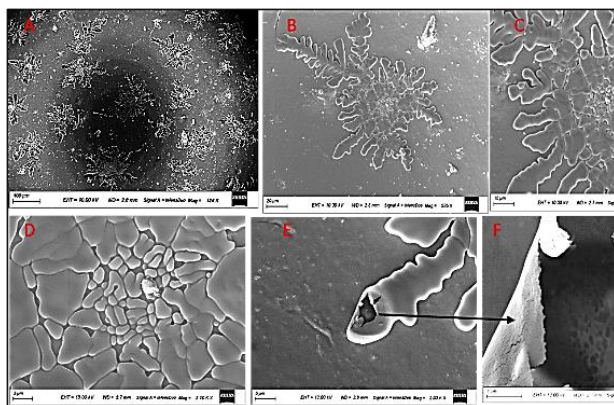


Figure (3) Morphology of CZTS film synthesized by sol-gel technique before sulfurization (annealing process)

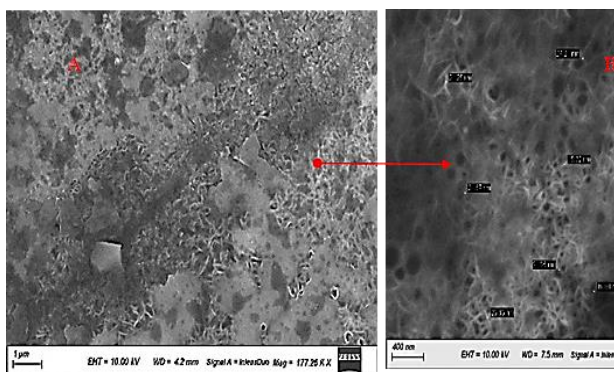


Figure (4) SEM images of CZTS film synthesized by sol-gel technique sulfurization (annealing process)

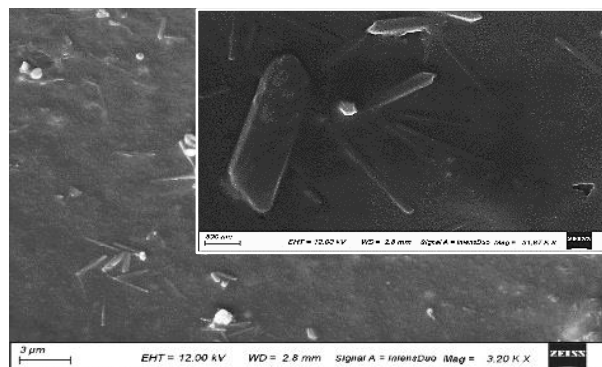


Figure (5) SEM images of ZnS secondary phases in CZTS film synthesized by sol-gel technique, at PH8.

### Acknowledgment

This paper is based upon work supported by Science, Technology & Innovation Funding Authority (STDF) under the grant (YRG Call 9), project ID (33421).

### 5. Conclusion

The preparation technique has a key role in the final characteristics of the CZTS kesterite layer. There is a strong connection between the resulting layer morphology, structure, and electrical properties. For example, the absence of secondary phases on the CZTS layers produced by the spray pyrolysis technique leads to high conductive characteristics. Also, the sulfurization process enhanced the carriers’ concentration by several orders of magnitude as well as the conductivity values for those samples prepared by the Sol-gel technique.

### List of abbreviation

(CZTS): Copper zinc tin sulfide, kesterite.  
(CdTe): Cadmium telluride.  
(XRD): X-ray diffraction patterns.  
(SEM): Scanning electron microscope.

### Availability of Data and Materials

All data generated or analysed during this study are included in this published article [and its supplementary information files.

### Conflict of Interest Statement

This work has no conflict of interest.

### References:

1. S. Delbos, EPJ Photovoltaics 3, 35004 (2012).
2. A. H. Ibrahim, L. Saad, A. A. Said, M. Soliman and S. Ebrahim, AIP Advances 12 (1), 015007 (2022).

3. Z. Oulad Elhmaidi, M. Abd-Lefdil and M. A. El Khakani, *Nanomaterials* 10 (7), 1393 (2020).
4. R. Aruna-Devi, M. Latha, S. Velumani and J. Á. Chávez-Carvayar, *Rare Metals* 40, 2602-2609 (2021).
5. N. S. Seroka, R. Taziwa and L. Khotseng, *Materials* 15 (15), 5338 (2022).
6. G. Magdy, M. E. Harb, A. Elshaer, L. Saad, S. Ebrahim and M. Soliman, *Jom* 71, 1944-1951 (2019).
7. S.-Y. Kuo and M.-Y. Hsieh, *Nanoscale* 6 (13), 7553-7559 (2014).
8. S. Tripathi, P. Lohia and D. Dwivedi, *Solar Energy* 204, 748-760 (2020).
9. B. Shin, T. Gershon and S. Guha, *Copper Zinc Tin Sulfide-Based Thin-Film Solar Cells*, 335-361 (2014).
10. H.-J. Jeong, Y.-C. Kim, S.-T. Kim, M.-H. Choi, Y.-H. Song, J.-H. Yun, M.-S. Park and J.-H. Jang, *Micromachines* 11 (9), 877 (2020).
11. T. Ratz, G. Brammertz, R. Caballero, M. León, S. Canulescu, J. Schou, L. Gütay, D. Pareek, T. Taskesen, D. H. Kim, J. K. Kang, C. Malerba, A. Redinger, E. Saucedo, B. Shin, H. Tampo, K. Timmo, N. D. Nguyen and B. Vermang, *Journal of Physics: Energy* 1 (4), 042003 (2019).
12. U. Saha and M. K. Alam, *RSC Advances* 8 (9), 4905-4913 (2018).
13. M. Jiang and X. Y., (2013).
14. A. Guchhait, Z. Su, Y. F. Tay, S. Shukla, W. Li, S. W. Leow, J. M. R. Tan, S. Lie, O. Gunawan and L. H. Wong, *ACS Energy Letters* 1 (6), 1256-1261 (2016).
15. S. Patel and J. V. Gohel, presented at the International Conference on Sustainable Development for Energy and Environment, India, 2017 (unpublished).
16. O. Awadallah and Z. Cheng, *IEEE Journal of Photovoltaics* 6 (3), 764-769 (2016).
17. T. R. Rana, N. Shinde and J. Kim, *Materials Letters* 162, 40-43 (2016).
18. E. Mkawi, K. Ibrahim, M. Ali, K. Saron, M. Farrukh and N. K. Allam, *Journal of Materials Science: Materials in Electronics* 26, 222-228 (2015).
19. N. Muhunthan, O. P. Singh, S. Singh and V. Singh, *International Journal of Photoenergy* 2013 (2013).
20. N. Muhunthan, O. P. Singh, M. Thakur, P. Karthikeyan, D. Singh, M. Saravanan and V. Singh, *J. Solar Energy* 2014, 1-2 (2014).
21. F. Hergert and R. Hock, *Thin solid films* 515 (15), 5953-5956 (2007).